NANO LETTERS

Letter

Magnetotransport in Co-Doped ZnO Nanowires

Wenjie Liang, Benjamin D. Yuhas, and Peidong Yang

Nano Lett., **2009**, 9 (2), 892-896• DOI: 10.1021/nl8038184 • Publication Date (Web): 26 January 2009

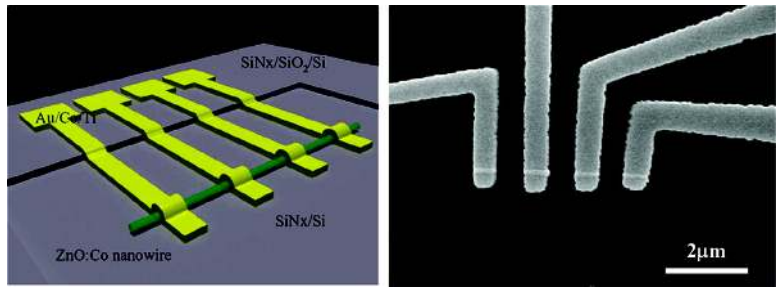

More About This Article

Additional resources and features associated with this article are available within the HTML version:

- Supporting Information
- Access to high resolution figures
- Links to articles and content related to this article
- Copyright permission to reproduce figures and/or text from this article

View the Full Text HTML

Nano Letters is published by the American Chemical Society. 1155 Sixteenth Street N.W., Washington, DC 20036

NANO LETTERS

2009
Vol. 9, No. 2
892-896

Magnetotransport in Co-Doped ZnO Nanowires

Wenjie Liang, Benjamin D. Yuhas, and Peidong Yang*

Department of Chemistry, University of California, Berkeley, California 94720

Received December 18, 2008; Revised Manuscript Received January 14, 2009

ABSTRACT

Electrical and magnetotransport measurements were performed on individual Co-doped ZnO dilute magnetic semiconductor nanowires. The electron transport studies show that the electron mobility could be as high as 75 $cm^2/(V·s)$, and we observed positive magnetoresistivity (MR) at low magnetic field and negative MR at higher magnetic field. s−d exchange-induced spin splitting of the conduction band could account for positive MR while suppression of weak localization of impurity centers could account for the negative MR. Lowering the carrier concentration in these nanowires through the application of a gate voltage tends to induce a larger magnitude MR as well as additional fine structure in the MR curves.

Spintronics has emerged as a promising field for future semiconductor devices.[1,2] The ability to manipulate both the spin and charge degrees of freedom is necessary to realize advanced functionality in these devices. Recently, dilute magnetic semiconducting (DMS) materials have generated extraordinary research interest due to their potential as ideal materials for spintronic devices. In DMS materials, the collective magnetic ordering has been shown theoretically[3] and experimentally[4,5] to be mediated by the semiconductor charge carriers, as well as electron scattering at localized magnetic impurities and electron−electron interactions. The ferromagnetic ordering in these systems could then lead to spin-polarized charge transport.[6−8] Electrostatic control of magnetization has been demonstrated in Mn-doped InAs and GaAs thin films;[9] however, the Curie temperature (T_C) of these materials remains far below room temperature. For practical applications, T_C must be above 300 K. Transition metal (TM) doped wide band gap semiconductors, such as ZnO or GaN, are theoretically predicted to have T_C above 300 K,[3] so they could be potential material candidates for practical spintronic devices. In the past, room temperature ferromagnetism has been experimentally demonstrated in Co- or Mn-doped ZnO[10] thin films, although the origin of the observed magnetic properties in TM-doped ZnO materials is still quite controversial[11] and further investigation of charge and spin transport through these materials is needed. In addition, the majority of magnetotransport studies on DMS materials have been in either the bulk or thin film forms. There are far fewer reports of spin transport in lower-dimensional DMS materials, such as nanowires.

In this Letter, we report electron transport and magnetoresistance studies of Co-doped ZnO nanowires. Pure and TM-doped ZnO nanowires were synthesized with a solution phase method, using $Zn(OAc)_2$ and $M(OAc)_2$ (M = Co, Mn, Fe, or Cu) as precursors. Detailed experimental information has been published elsewhere.[12] Using this method, pure and TM-doped ZnO nanowires with various doping concentrations could be synthesized. In this study, we focused on ZnO nanowires with 10% (atomic) Co doping (Figure 1a,b).

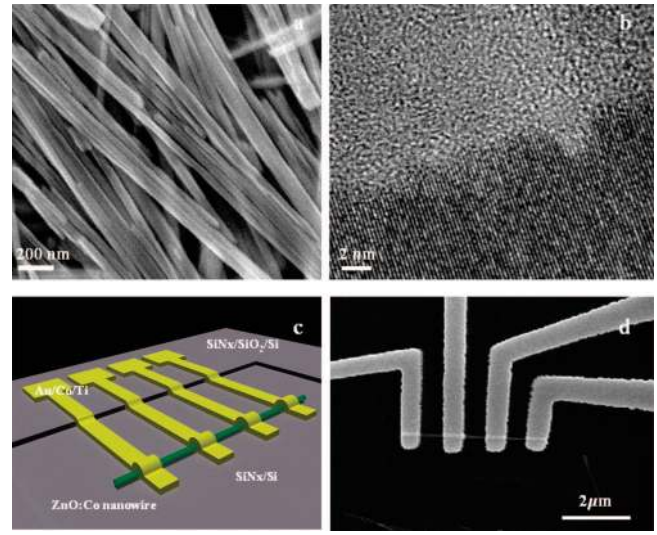

Figure 1. (a) SEM image of as-made Co-doped ZnO nanowires. (b) HRTEM of a Co-doped ZnO nanowire. (c) Schematic drawing of Co-doped ZnO nanowire device layout (not to scale). Devices were made on Si with a 600 nm SiO_2 layer. The center area is etched, and a 50 nm Si_xN_y layer was deposited. Co-doped ZnO nanowires lie directly on the Si_xN_y film. Contact metals are 1 nm/100 nm/30 nm Ti/Co/Au, respectively. (d) SEM image of individual Co-doped ZnO nanowire with four electrical contacts.

The nanowires were dispersed in ethanol and spin-cast onto premade substrates for transport studies. The substrates were made such that 100 μm by 100 μm windows were

10.1021/nl8038184 CCC: $40.75
Published on Web 01/26/2009

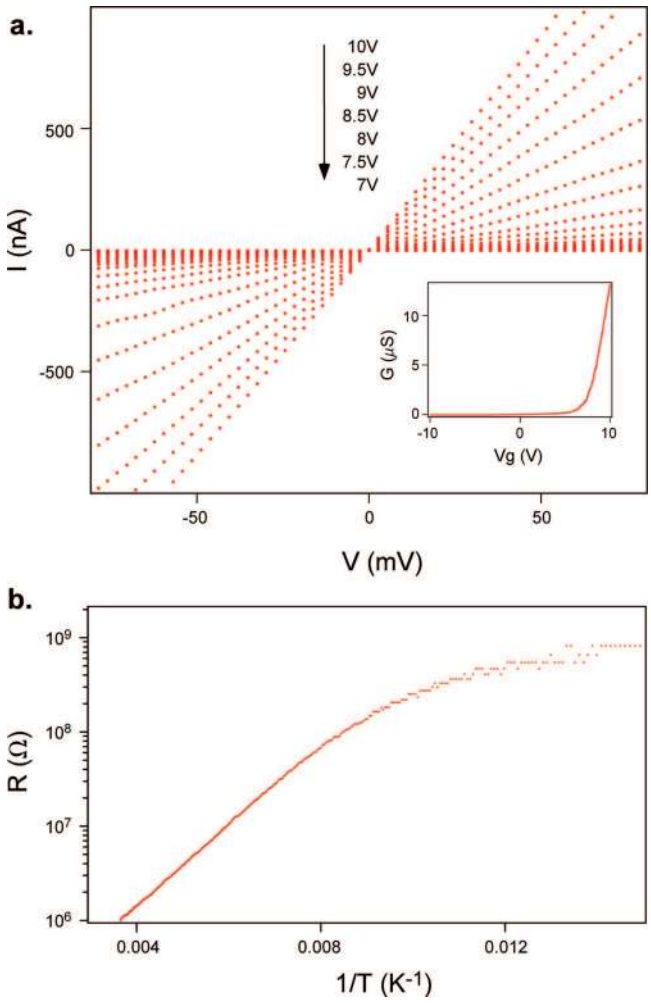

Figure 2. Electron transport measurement of a single Co-doped ZnO nanowire. (a) $I-V$ curves taken at different gate voltages, V_g. The most conductive $I-V$ curve was from $V_g = 10$. Each curve below is taken at different gate voltage with 0.5 V interval. Inset: Conductance vs V_g plot for the same device. (b) Temperature-dependent resistance of the device.

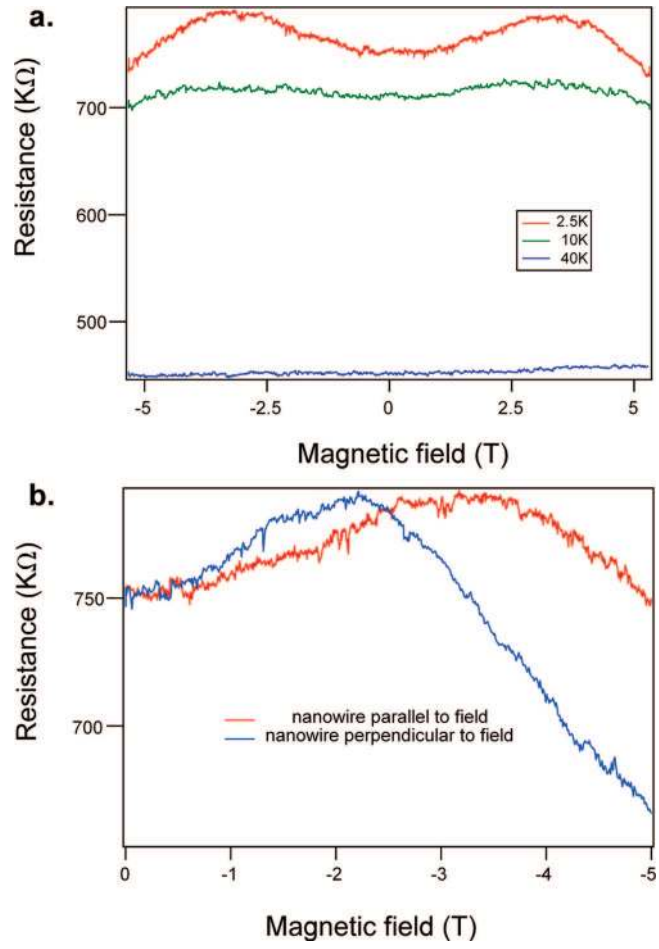

Figure 3. Magnetoresistance measurement at (a) different temperatures and (b) different field orientations taken at 2.5 K and 29 V gate voltage.

opened on a 600 nm thick SiO_2 covered Si chip. Then, 50 nm of Si_xN_y was grown on the surface so that the deposited ZnO nanowires would lie directly on the Si surface with only 50 nm Si_xN_y as spacer (Figure 1c,d). The substrates were prepared with alignment markers so standard e-beam lithography could be performed to define electrical contacts to individual nanowires. 1 nm/100 nm/20 nm Ti/Co/Au were deposited as electrode materials in an e-beam evaporator after the nanowire surface was cleaned in an O_2 plasma cleaner for 30 s at a power of 50 W.

Room temperature electron transport measurements were performed in a Faraday cage with a multifunctional DAC card (National Instrument 6052E) as voltage sources and signal collecting unit. Low-temperature and magnetotransport measurements were performed in a superconducting quantum interference device (SQUID) and a cryostat with a split coil superconducting magnet so that the sample could be rotated with respect to the magnetic field direction. A Keithley (model 236) source-measurement unit, a Stanford Research System lock-in amplifier (SR810), and a Digital Instrument current preamplifer (DL-1211) were used for the low-temperature measurements.

Panels a and b of Figure 1 show scanning electron microscopy (SEM) and high-resolution transmission microscopy (HRTEM) images of representative Co-doped ZnO nanowires we used for our studies. As-made Co-doped ZnO nanowires have a diameter of 35 ± 5 nm and length up to 5 μm. HRTEM image (Figure 1b) shows that these Co-doped ZnO nanowires are single crystalline. Further careful examination confirmed that these nanowires possess a uniform doping profile with no detectable secondary phases or dopant concentration gradients.[13] This makes our Co-doped ZnO nanowires an ideal candidate for magnetotransport studies in TM-doped ZnO materials. Collective magnetization measurements, presented previously,[13] indicate that the nanowires have a weak ferromagnetism that persists up to room temperature, with a paramagnetic component dominating at low temperature.

For our magnetotransport studies, we made two-probe current (I)−voltage (V) measurements and four-probe (Figure 1, panels c and d) $I-V$ measurements on individual 10% Co-doped ZnO nanowires. The majority of our devices show linear $I-V$ curves with two-probe and four-probe resistances that differ by less than 1%, which suggests that we have Ohmic contact to the nanowires and that contact resistance

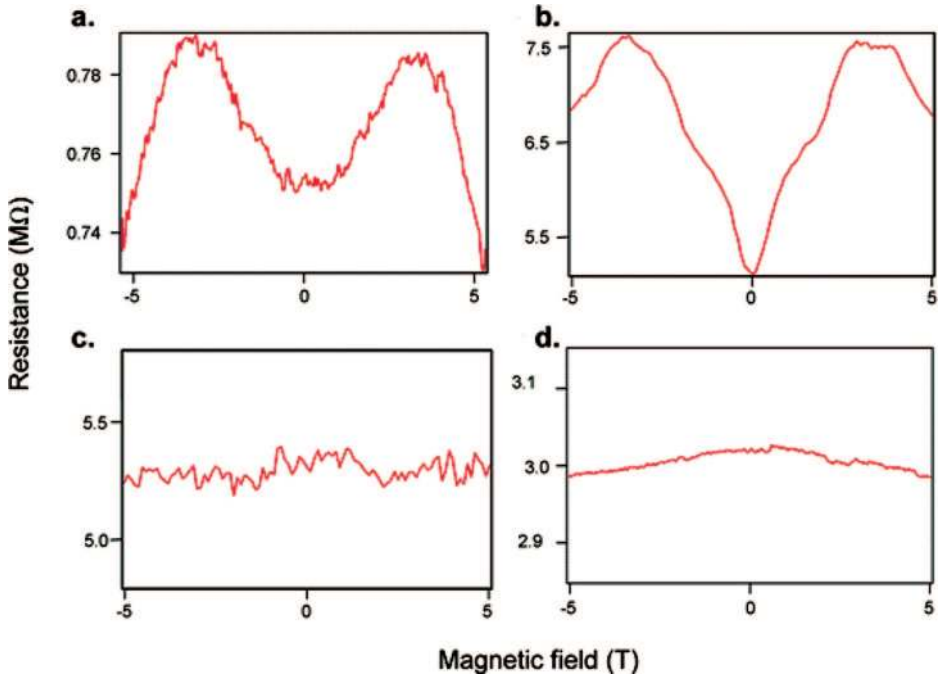

Figure 4. Magnetoresistance measurements for (a) Co contact to Co-doped ZnO nanowire; (b) Au contact to Co-doped ZnO nanowire; (c) Co contact to pure ZnO nanowire, and (d) Au contact to pure ZnO nanowire. Control devices b−d were tuned to have comparable resistivities. The temperature for all measurements was 10 K.

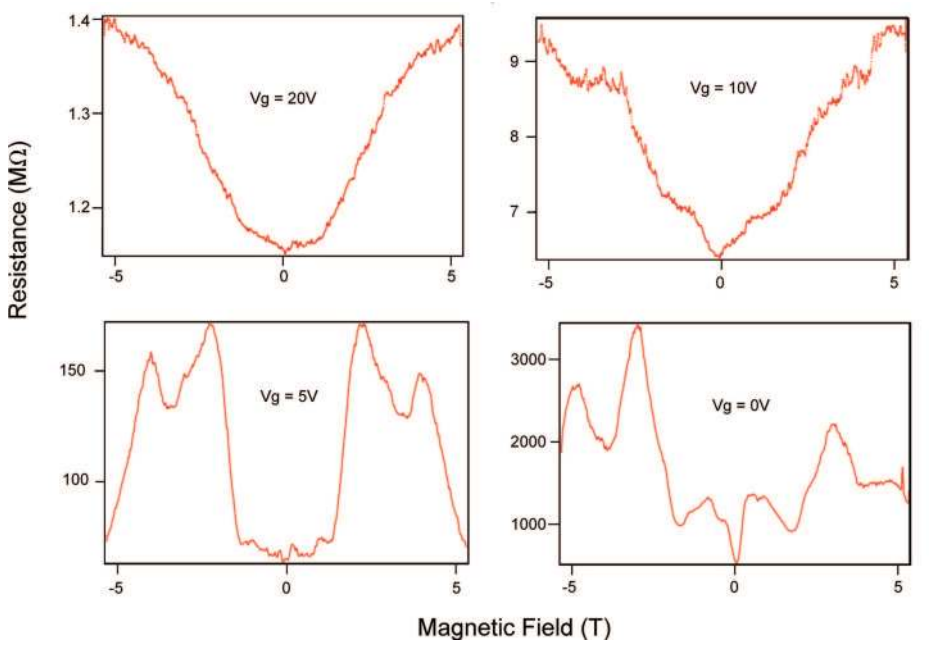

Figure 5. Gate-voltage-dependent MR for a ZnO:Co nanowire device, measured at 2.5 K.

is negligible. Figure 2a shows two-probe $I-V$ curves taken with different applied gate voltages, V_g (−10 to 10 V with a step size of 0.5 V). The conductance, G, increases with increasing gate voltage, indicating n-type conduction. The inset shows the nanowire conductance versus V_g. The device is turned on when positive gate voltage is applied and the conductance increases with V_g. The electron mobility is calculated from the transconductance, dG/dV_g, and from the geometry of the nanowire.[14] We estimate the electron mobility in our Co-doped ZnO nanowires to be on the order of tens of cm^2/(V•s), with the highest value to be 75 cm^2/(V•s). This number is comparable to the best-reported mobilities of n-type ZnO materials. The carrier concentration is on the order of $(2-5) \times 10^{18}$ cm^{-3}. This suggests that the Co dopants do not drastically decrease the mobility due to their similar ionic radii. In a previous publication,[13] we reported that our doping process occurs with a high degree of order retained in the nanowires; there are no widespread defects or dislocations in the ZnO lattice as a result of TM dopant incorporation. This high degree of order gave rise to a relatively weak ferromagnetic coupling, as predicted by theory.[14,15] We thus see that our ordered doping process,

although yielding weaker ferromagnetism, endows our nanowires with well-defined intrinsic transport properties and that both the observed electronic and magnetic behavior can be explained by a common mechanism.

The resistance of the nanowires was measured at temperature between 5 and 300 K. The temperature-dependent resistance plot (Figure 2b) shows the resistance of a single nanowire plotted in a logarithmic scale as a function of reciprocal temperature $1/T$. In the simplest modeling, $\log R$ can be written as

$$\log R = E_a/k_bT + \text{constant}$$

where E_a is the activation energy that electrons need to overcome to hop into the conduction band of the ZnO nanowires and k_B is the Boltzmann constant. Fitting our data of doped ZnO nanowires, we found that E_a varies from 38 to 45 meV.

Figure 3 represents one of our typical magnetotransport measurements. In Figure 3a, magnetoresistance (MR) was recorded as a function of magnetic field (B) at different temperatures. The axial direction of the nanowire was aligned with the magnetic field. After the nanowire was slowly cooled down to 2.5 K, resistance was monitored using a lock-in amplifier while magnetic field was swept between −5 and 5 T. Interestingly, the measured MR as a function of magnetic field is not monotonic. Positive MR was observed with small B, and when B is further increased, a maximum MR was reached. A further increase in B results in decreasing MR. Negative MR could be observed at high values of B. The measured maximum positive MR (R_{max}) is 5%, occurring at a turnover field of 3.3 T. At 5 T, MR drops by 5% compared to R_{max}. This phenomenon of MR reversal was repeatedly observed in all other Co-doped ZnO nanowires we tested, although the turnover field where the maximum MR was observed differs slightly from sample to sample. In some cases, we only observed a shoulder up to 5 T. The highest MR achieved was 24%. The temperature dependence of the MR was also presented in Figure 3a. The magnitude of the MR decreases as the temperature increases, with noticeable MR vanishing above 40 K.

Figure 3b shows MR plots at 2.5 K as a function of magnetic field orientation relative to the c axis of the nanowire. When the field direction changed from parallel to c axis to perpendicular to it, the general observed MR versus field curve shape remains the same, but the turnover field decreases from 3.3 to 2.1 T, and a greater negative MR was observed at high field (∼20% compared with R_{max}). The reduction of turnover field upon sample rotation, as well as the larger negative MR at high field, was observed in multiple devices. These observations suggest that perpendicular field favors negative MR. One plausible reason might be that the hard axial direction for magnetizations is along the nanowire direction; this has been shown in numerous EPR and bulk magnetization measurements.[16] No significant MR hysteresis was observed when the field sweeping direction was changed.

To confirm that the observed MR indeed arises from Co doping in the ZnO lattice, additional nanowire devices were tested: (1) Au-contacted Co-doped ZnO nanowires, (2) Co-contacted pure ZnO nanowires, and (3) Au-contacted pure ZnO nanowires. The changing of MR from positive to negative direction was also observed in Au-contacted Co-doped ZnO nanowires, but it is clearly absent in MR plots of both Co-contacted pure ZnO nanowires and Au-contacted pure ZnO nanowires (Figure 4). Interestingly, we note that our Au-contacted pure ZnO nanowires showed a small negative MR, the origin of which is still unclear at this point. Nevertheless, the above control experiments show that our observed MR behaviors in our Co-doped ZnO nanowires are intrinsic properties to the doped nanowires themselves.

In n-type ZnO, the conduction band is primarily comprised of s electrons. The introduction of a transition metal impurity can induce a spin-split conduction band due to s−d exchange interaction. Electron redistribution between the two subbands in the presence of a magnetic field leads to positive MR due to relaxation time changes for electrons at the Fermi surfaces.[15] The electron spin-disorder scattering is also favorable for a low-temperature/low field positive MR.[6,17] When the temperature is raised, the Fermi energy becomes much larger than the energy difference between the subbands, so the difference of the electron populations in the two subbands would be negligible.[18−20] Thus, the positive MR becomes weaker as temperature increases. At higher magnetic fields, the negative MR observed could be attributed to the suppression of weak localization of impurity centers. In higher magnetic fields, the alignment of the Co magnetic moment and more polarized spin current lead to non-negligible reduction of electron scattering and hence resistance, contributing to the turnover of the MR curves.[18] The observation of positive and negative MR in our Co-doped ZnO nanowire device is the result of the competition between these two physical processes. Similar behavior was also previously observed in pulse laser deposition (PLD) prepared Co-doped thin films.[6,20−22]

Since the carrier concentration of the host semiconductor can greatly influence DMS material magnetic properties, it is interesting to study the MR of the same nanowire at different carrier concentrations. The carrier concentration can simply be tuned by the application of a gate voltage. Figure 5 shows the MR of a Co-doped ZnO nanowire while its conductance was tuned by back gating. In general, the magnitude of the MR increases when the conduction electrons are slowly depleted, i.e., as gate voltage decreases. The positive MR magnitude increased from 20% to 48% to 120% to 300% while the gate voltage was lowered from 20 V to 10 V to 5 V to 0 V. The increase of positive MR could be a result of more spin-polarized current at lower conduction electron concentrations. As temperature was increased, MR persists at higher temperature when gate voltage was tuned more negatively. Curiously, at lower gate voltages, the MR curve shapes become much more complex, with shoulders and multiple peaks as the applied field was modulated. These subtle features could be related to fine details in the band structure and additional spin scattering processes at the impurity centers, although further research is necessary to confirm this hypothesis. Similar MR behavior was previously observed in Co-doped ZnO thin films,[20] and we believe that

this is the first report of such anomalous MR in Co-doped ZnO nanowires.

To summarize, electrical and magnetotransport measurements were performed on individual Co-doped ZnO nanowires. The electron transport studies show that the electron mobility could be as high as 75 $cm^2/(V•s)$, and we observed positive MR at low magnetic field and negative MR at higher magnetic field. s−d exchange-induced spin splitting of the conduction band could account for positive MR while suppression of weak localization of impurity centers could account for the negative MR. Lowering the carrier concentration in these NWs through the application of a gate voltage tends to induce a larger magnitude MR as well as additional fine structure in the MR curves. Our results represent the first magnetotransport experiments for high-quality Co-doped ZnO nanowires, and through these and future efforts, we seek to attain a better understanding of the mechanism of magnetic ordering in DMS nanowires that will ultimately lead to the construction of practical spintronic devices.

Acknowledgment. We thank WIN for funding support and Professor Frances Hellman for the use of their SQUID. We thank Dr. Rong Fan for SiN_x substrate preparation. We thank Dr. Ajey Jacob and Dmitri Nikonov for thoughtful discussion.

References

(1) Wolf, S. A.; Awschalom, D. D.; Buhrman, R. A.; Daughton, J. M.; von Molnár, S.; Roukes, M. L.; Chitchelkanova, A. Y.; Treger, D. M. *Science* **2001**, *294*, 1488.
(2) Awschalon, D. D.; Flatte, M. E. *Nat. Phys.* **2007**, *2*, 153.
(3) Ditel, T.; Ohno, H.; Matsukura, F.; Clbert, J.; Ferrand, D. *Science* **2000**, *287*, 1019.
(4) Ohno, Y.; Young, D. K.; Beschoten, B.; Matsukura, F.; Ohno, H.; Awschalom, D. D. *Nature* **1999**, *402*, 790.
(5) Tanaka, M.; Higo, Y. *Phys. Rev. Lett.* **2001**, *87*, 026602.
(6) Xu, Q.; Hartmann, L.; Zhou, S.; Mcklich, A.; Helm, M.; Biehne, G.; Hochmuth, H.; Lorenz, M.; Grundmann, M.; Schmidt, H. *Phys. Rev. Lett.* **2008**, *101*, 076601.
(7) Rüster, C.; Borzenko, T.; Gould, C.; Schmidt, G.; Molenkamp, L. W.; Liu, X.; Wojtowicz, T. J.; Furdyna, J. K.; Yu, Z. G.; Flatté, M. E. *Phys. Rev. Lett.* **2003**, *91*, 216602.
(8) Choi, H.; et al. *Adv. Mater.* **2005**, *17*, 1348.
(9) Ohno, H.; Chiba, D.; Matsukura, F.; Omiya, T.; Abe, E.; Dietl, T.; Ohno, Y.; Ohtani, K. *Nature* **2000**, *408*, 944.
(10) Bouloudenine, M.; Viart, N.; Colis, S.; Kortus, J.; Dinia, A. *Appl. Phys. Lett.* **2005**, *87*, 052501.
(11) Coey, J. M. D.; Chambers, S. A. *MRS Bull.* **2008**, *33*, 1053.
(12) Yuhas, B.; Zitoun, D. O.; Pauzauskie, P. J.; He, R.; Yang, P. *Angew. Chem., Int. Ed.* **2006**, *45*, 420.
(13) Yuhas, B.; Fakra, S.; Marcus, M. A.; Yang, P. *Nano Lett.* **2007**, *7*, 905.
(14) Berciu, M.; Bhatt, R. N. *Phys. Rev. Lett.* **2001**, *87*, 107203.
(15) Coey, J. M. D.; Venkatesan, M.; Fitzgerald, C. B. *Nat. Mater.* **2005**, *4*, 173.
(16) Venkatesan, M.; Fitzgerald, C. B.; Lunney, J. G.; Coey, J. M. D. *Phys. Rev. Lett.* **2004**, *93*, 177206.
(17) Shapira, Y.; Kautz, R. L. *Phys. Rev. B* **1974**, *10*, 4781.
(18) Lee, P. A.; Ramakrishnan, T. V. *Rev. Mod. Phys.* **1985**, *57*, 287.
(19) Budhani, R. C.; Pant, P.; Rakshit, R. K.; Senapati, K.; Mandal, S.; Pandey, N. K.; Kumar, J. *J. Phys.: Condens. Matter* **2005**, *17*, 75.
(20) Xu, Q.; Hartmann, L.; Schmidt, H.; Hochmuth, H.; Lorenz, M.; Schmidt-Grund, R.; Sturm, C.; Spemann, D.; Grundmann, M. *Phys. Rev. B* **2006**, *73*, 205342.
(21) Xu, Q.; et al. *Thin Solid Films* **2006**, *515*, 2549.
(22) Dietl, T.; Andrearczyk, T.; Lipińska, A.; Kiecana, M.; Tay, M.; Wu, Y. *Phys. Rev. B* **2007**, *76*, 155312.

NL8038184